



## OPEN ACCESS

EDITED BY  
Hongbo Cong,  
University of Akron, United States

REVIEWED BY  
Biao Zhao,  
Nanjing University of Aeronautics and  
Astronautics, China  
Chongjun Wu,  
Donghua University, China

\*CORRESPONDENCE  
Guijian Xiao,  
✉ xiaoguijian@cqu.edu.cn

SPECIALTY SECTION  
This article was submitted to  
Environmental Degradation of Materials,  
a section of the journal  
Frontiers in Materials

RECEIVED 24 September 2022  
ACCEPTED 30 November 2022  
PUBLISHED 13 December 2022

CITATION  
Jiang G, Yang H, Xiao G, Zhao Z and  
Wu Y (2022), Titanium alloys surface  
integrity of belt grinding considering  
different machining trajectory direction.  
*Front. Mater.* 9:1052523.  
doi: 10.3389/fmats.2022.1052523

COPYRIGHT  
© 2022 Jiang, Yang, Xiao, Zhao and Wu.  
This is an open-access article  
distributed under the terms of the  
[Creative Commons Attribution License  
\(CC BY\)](https://creativecommons.org/licenses/by/4.0/). The use, distribution or  
reproduction in other forums is  
permitted, provided the original  
author(s) and the copyright owner(s) are  
credited and that the original  
publication in this journal is cited, in  
accordance with accepted academic  
practice. No use, distribution or  
reproduction is permitted which does  
not comply with these terms.

# Titanium alloys surface integrity of belt grinding considering different machining trajectory direction

Guiyun Jiang, Hang Yang, Guijian Xiao\*, Zeyong Zhao and Yuan Wu

College of Mechanical and Vehicle Engineering, Chongqing University, Chongqing, China

The interplay of abrasive grains and materials complicates the grinding of titanium alloys by abrasive belts. Notably, the influence relationship of surface generation for complex curved workpieces such as hollow blades needs to be clarified, making precise control of the surface integrity of complex surfaces difficult in abrasive belt grinding applications. This paper thus proposes a trajectory planning method based on the direction of interaction between grinding grains and materials to reveal its influence law on the surface integrity of complex curved surfaces of titanium alloy with unevenly distributed machining allowances. First, a machining trajectory with different angles between the grinding direction and feed direction is proposed. In order to determine the corresponding experimental scheme for titanium alloy hollow blades. Experimental results are used to analyze the influence of different grinding trajectory directions on the surface roughness, residual stress, surface topography, and accuracy of the contours. The results show that different grinding trajectory directions significantly affect the workpiece's surface integrity. By varying the grinding trajectory direction, it is possible to reduce the surface roughness of titanium alloy workpieces by approximately 40%, increase the surface residual compressive stress by approximately 50%, provide a finer workpiece surface and improve the consistency of the surface texture. This work is expected to guide the efficient and high-quality machining of complex curved parts such as titanium alloy hollow blades.

## KEYWORDS

titanium alloy, belt grinding, complex surfaces, surface integrity, trajectory direction

## 1 Introduction

Titanium alloy TC4, a metallic material with high specific strength, high fracture toughness, and good heat and corrosion resistance, has been widely used to fabricate essential components in aviation, aerospace, shipping, and wind energy. However, because of its low thermal conductivity, high chemical activity, and low elastic modulus, titanium alloys are subject to flaws such as burns on the workpiece surface, causing severe tool wear and deformation due to rebound during machining

(Liang et al., 2020; Pushp et al., 2022; Xu et al., 2022). Belt grinding technology with cold and elastic characteristics can process nearly all engineering materials. It plays an essential role in the machining process of some of the critical components of major equipment in advanced manufacturing technology (Sabarinathan et al., 2020; Zhu and Beaucamp, 2020; Li et al., 2022). For this reason, the industry commonly uses belt grinding and polishing for the final surface treatment of complex curved parts such as hollow titanium blades to regulate their surface integrity. Surface roughness, residual stress, and microhardness are critical indicators of the surface's integrity and significantly impact the machining quality and serviceability of titanium alloy hollow blades (Kalantari et al., 2021; Rangasamy et al., 2022; Liu et al., 2023). During belt grinding, abrasive grains come into contact with the workpiece surface and are coupled with a variety of actions such as pressing, scraping, ploughing, and cutting in order to achieve material removal or plastic deformation of the machined surface (Li et al., 2021; Palaniyappan et al., 2022; Zhu et al., 2022). The trajectory of abrasive belt motion during grinding is thus closely related to surface creation. Understanding the influence of abrasive belt grinding surface integrity is vital for improving the surface quality and service performance of complex curved workpieces such as titanium alloy blades.

Many researchers have extensively researched the surface integrity of complex surface machining of titanium alloys. Guo et al. (2019) proposed a multi-objective method for optimising process parameters. Through the experimental study of belt polishing, they achieved the optimum parameter combination, which may reduce the surface roughness and improve the material removal rate. Zhang et al. (2022) analysed the finite element model and pressure distribution of blade contact, extracted polishing curves using NURBS curves, and considered trajectory planning based on the flexible contact deformation of the blade surface. It can reduce surface roughness and improve polishing efficiency. The effect of grinding process parameters on workpiece surface integrity was analysed. The workpiece surface integrity was better under the same process parameters than conventional high-speed grinding (Yi et al., 2019). Tao et al. (2017) studied the effect of grinding parameters such as cutting speed, feed rate, grinding depth, and abrasive size on integrity of the surface experimentally. According to a residual stress forecasting model developed using multiple regression, Chen et al. (2019) studied and found the optimum parameter range for the ranges of maximum and stable residual stresses. For example, Tan et al. (2020) A study of the surface integrity pattern of TC17 blades under the integrated manufacturing process route showed that they had lower surface roughness, smoother surface profile, greater compressive residual stress, and surface microhardness following vibration polishing treatment. Liu et al. (2020) investigated the effect of process parameters on the relationship between abrasive chip shape and surface

topography. They analysed the effect of process parameters on surface roughness and residual stress, comparing the change in surface integrity before and after blade machining.

To conclude, researchers have conducted numerous studies on aspects related to the surface integrity of the complex surface machining of titanium alloys. However, relevant journals and reports have yet to reveal the law of influence of different trajectory planning directions on titanium alloys' surface integrity during belt grinding. Therefore, this paper takes TC4 titanium alloy as the research object and proposes a trajectory planning method based on the interaction direction between the abrasive belt grit and the material, with a  $\theta$  angle between the abrasive belt grinding direction and the feed direction, and uses different grit sizes of abrasive belts for relevant experiments. By analysing the grinding test results of titanium alloy hollow blades. To reveal the influence law of the relationship between grinding direction and feed direction on the surface integrity, such as surface roughness, residual stress, surface topography, and contour accuracy of titanium alloy samples with an uneven distribution of machining allowances.

## 2 Experimental method

### 2.1 Materials and equipment

For the grinding tests, the hollow blades were made from TC4 titanium alloy, consisting of Ti-6Al-4V, a titanium alloy of the ( $\alpha + \beta$ ) type with good overall mechanical and mechanical properties. Due to its high strength and good process plasticity but low thermal conductivity, it quickly burns and forms corrugations during grinding (Hou et al., 2022). The specific chemical composition of TC4 titanium alloy and the specific chemical composition and mechanical property parameters of TC4 titanium alloy are shown in Table 1.

The experimental grinding equipment consists of a six-axis CNC machine tool and a particular fixture for grinding, as shown in Figure 1. This allows the machine to synchronize the six-axis motion according to the machining program and to achieve high-efficiency adaptive grinding of complex curved parts such as hollow blades.

### 2.2 Experimental scheme and trajectory planning method

Based on the team's previous experimental guidance on the optimization of grinding process parameters for fatigue-resistant surface abrasive belts for TC4 titanium alloy. In order to study the influence of abrasive belt grit size on the results obtained, the German VSM abrasive belt, CK772T model, was used for this grinding test, and three different grind sizes were chosen for comparison with the treatment. The same grinding process

**TABLE 1** Chemical composition and room temperature mechanical properties of TC4 titanium alloy.

Chemical composition	Fe	O	C	N	H	Al	V	Ti
Weight %	<0.30	<0.20	<0.10	<0.05	<0.015	5.5–6.8	3.5–4.5	The rest
Elastic Modulus/Gpa	Elongation/%	Section shrinkage/%	Density/kg·m <sup>-3</sup>	Tensile Strength/Mpa	Yield Strength/Mpa			
110	10	25	4510	902	824			

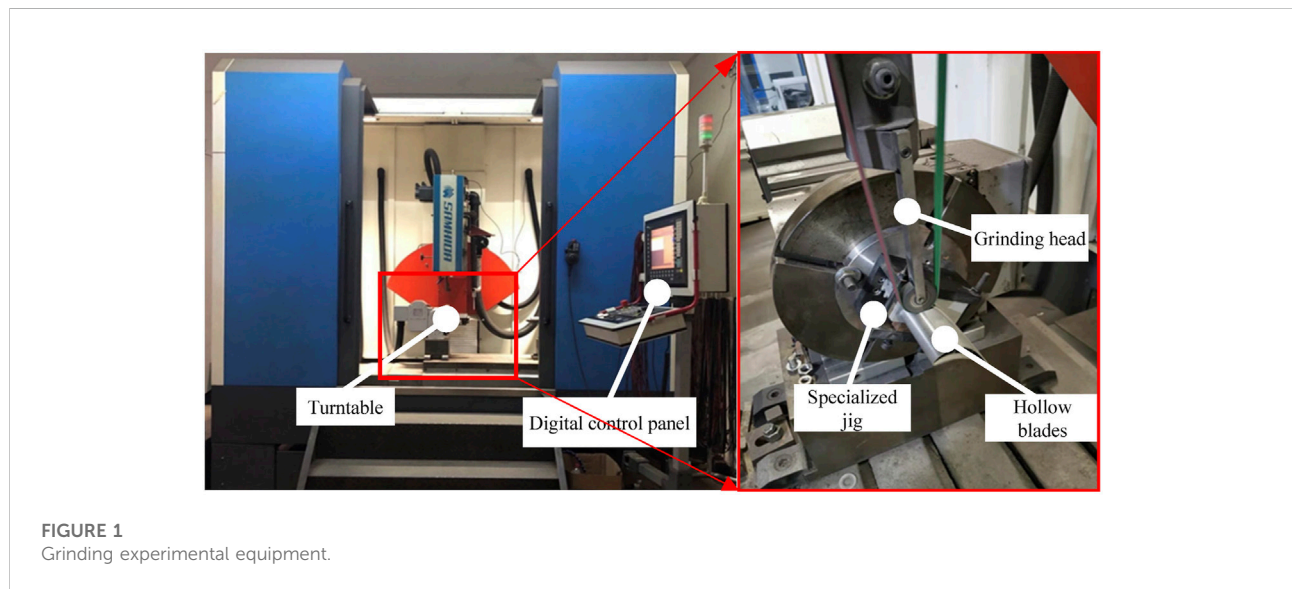


**FIGURE 1** Grinding experimental equipment.

**TABLE 2** Grinding process parameters for the experiments.

Belt material	Belt grain size	Average particle Size (μm)	Linear velocity (m/s)	Feedrate (mm/min)	Grinding depth (mm)	Step pitch (mm)
SiC	P400	35	13	120	0.1	2
	P600	25.8	13	120	0.1	2
	P800	21.8	13	120	0.1	2

**TABLE 3** Different angle  $\theta$ .

Angle between grinding direction and feeding direction of belt $\theta$ (°)						
0	30	45	60	90	0 + 90	

parameters were used for all three groups of experiments in order to achieve relatively stable experimental results, and the abrasive belt type was used. Grinding process parameters are presented in Table 2.

To investigate the interaction between the abrasive belt grit and the surface material of a titanium alloy hollow blade during the grinding process. This test proposes a trajectory planning method in which the belt grinding direction is at an angle  $\theta$  to the feed

direction. The CNC sets the starting and ending points of the grinding trajectory. The machining parameters specified in Tables 2, 3 (“0 + 90” stands for grinding at  $\theta = 0^\circ$  and then covering with  $\theta = 90^\circ$ ) are used to obtain a schematic diagram of the grinding trajectory for the blade test. Figure 2 illustrates the entry point, exit point, and movement path of the abrasive belt contact wheel, along with the actual grinding trajectory. The sample is fixed to the machine’s motion platform with a fixture during the grinding

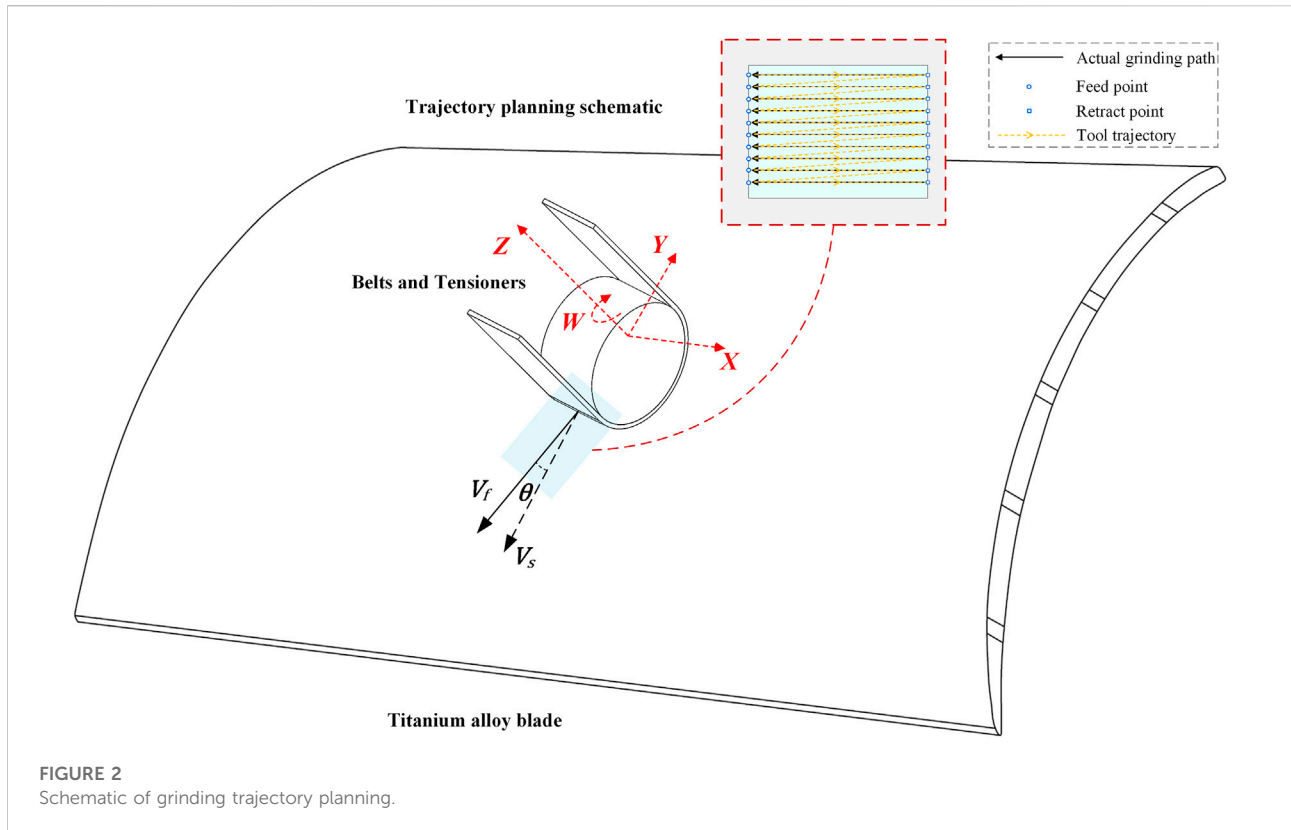


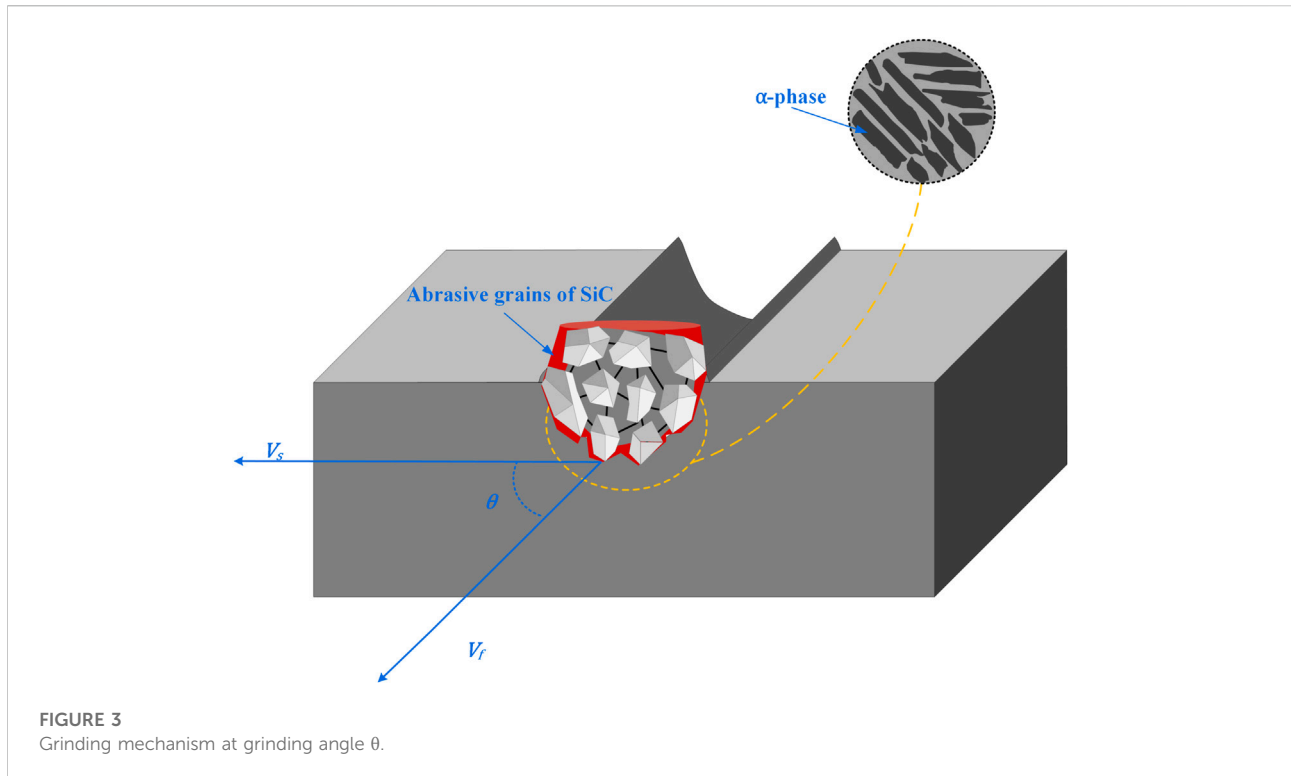
FIGURE 2  
Schematic of grinding trajectory planning.

process. The angle of the rotational axis  $W$  of the abrasive belt contact wheel is adjusted using the CNC panel so that the grinding speed  $V_s$  of the abrasive belt is at a  $\theta$  angle to the feed speed  $V_f$  of the sample during the actual grinding process.

Eight roughness measurement locations were randomly selected from each grinding zone before and after the grinding test. Surface roughness values were measured with a Form Talysurf Series 2 surface roughness measurement instrument perpendicular to the direction of the actual grinding trajectory. The sample length was set to 0.8 mm, the assessment length: was 4 mm, and the mean of the multiple measurements was used as the final measurement outcome. The grinding area was also cleaned of swarf and dust before measurement, and the sample curve of the area measured was held horizontally by adjusting the position of the sample placement to ensure the accuracy of the results.

Proto's LXR D high-speed vertical X-ray diffractometer with five measurement points set at 3 mm intervals over the grinding surface of the sample was used to perform the test, and residual stresses on the surface parallel to the actual direction of the grinding path were examined. The mean value was taken as the final measurement result. The equipment inspection parameters are as follows: tube voltage and tube current of 30 kV and 25 mA, respectively, of the target material of Cu-K $\alpha$ , the Ni target filter, selected {213} of the diffraction crystal plane and a diffraction angle of 142°.

The ( $\alpha + \beta$ ) type of titanium alloy consists of the  $\alpha$  and  $\beta$  phases forming the typical microstructure. Grinding treatment is an effective method for refining the grain and improving the wear resistance of the titanium alloy surface. Generating a refined and dense  $\alpha$ -phase layer can significantly enhance the overall performance of titanium alloying (Wang et al., 2021). Figure 3 shows that abrasive grains with a SiC substrate are brought into contact with the surface of the titanium alloy sample under a CNC device's control by coupling multiple scratching, pressing, and ploughing actions to achieve material removal from the titanium alloy sample. However, since TC4 titanium alloy contains many alpha-phases, the crystal orientation of the alpha-phase layer is arranged in a regular pattern, showing a certain angle to the grinding direction. During the grinding process, the abrasive grains interact with the surface of the titanium alloy, which is plastically deformed by the coupling of mechanical and high temperatures. As a result, once the angle  $\theta$  between the grinding direction and the feed direction is changed, the direction of interaction between the grinding grains and the  $\alpha$ -phase layer of the titanium alloy changes. This results in different slip or dislocation directions of the crystals in the  $\alpha$ -phase layer and the generation of grains with different orientations. It ultimately affects the direction and morphology of the surface texture generation of Ti-6Al-4V alloy during the grinding process.



As shown in Figure 4, different surface microtextures can be formed after processing the titanium alloy samples using different values of the angle  $\theta$ . Because of the different surface textures, the surface integrity of the ground titanium alloy samples can be quite different. Due to the variation in angle  $\theta$  between the grinding direction and the feed direction, the abrasive grains of the SiC matrix interact with the titanium alloy material to various degrees. Changes in the area and direction of the contact forces between the abrasive grains and the grooves result in the plastic formation of differently shaped grooves and pile-up of abrasive grains under the coupling of mechanical and thermal effects, thus causing different surface integrity. The flatness of the surface will first decrease and then increase as the angle  $\theta$  increases, with the highest flatness of the surface and the most uniform grinding texture at an angle of clamp  $\theta$  of  $0^\circ$ . As the angle  $\theta$  is increased to  $60^\circ$ , the flatness of the surface is lowest, and the grinding depth is deepest. For this reason, the feasibility and efficacy of the method are subsequently verified by adopting the clamping angle parameter  $\theta$  of  $0^\circ$  to perform abrasive belt grinding tests on titanium alloy hollow blades.

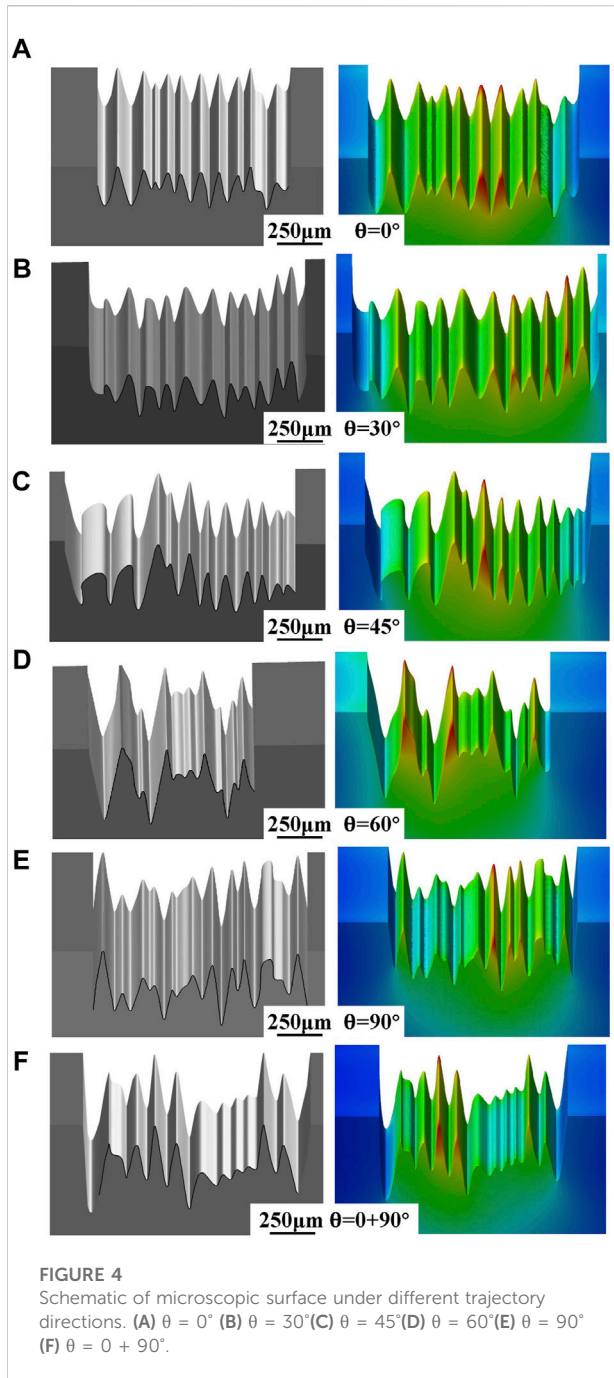
### 3 Results and discussion

#### 3.1 The effect of trajectory direction on surface roughness

Surface roughness has traditionally been used as an essential indicator of the integrity of the surface and can quantitatively

characterize the microscopic roughness of the machined surface. However, high surface roughness can easily lead to the development of fine cracks, which reduces the serviceability of titanium workpieces and hinders their routine use. Therefore, control of surface roughness is an essential goal in grinding operations, and surface roughness is currently the primary optimization goal for improving surface integrity (Lin et al., 2018). To ensure that the effect of varying  $\theta$  on the surface roughness met significance at the 0.05 level, all surface roughness data (Specific data shown in Supplementary Material) obtained from the measurements were divided into three groups by different belt grit sizes for tests of normality and a one-way ANOVA. Figure 5 shows the results of the post hoc ANOVA comparisons. These results indicate that there is indeed a significant difference in the level of surface roughness caused by the different values of  $\theta$ .

The mean values of the surface roughness measurements at different grit sizes of the abraded belts are shown in Figure 6. The surface roughness of the titanium alloy samples varied from Ra 0.31–0.44  $\mu\text{m}$  at the P400 grit size after the abrasive belt grinding process, from Ra 0.21–0.38  $\mu\text{m}$  at the P600 grit size, and from Ra 0.23–0.35  $\mu\text{m}$  at P800 grit size. As the angle  $\theta$  between the belt grinding direction and the feed direction of the titanium alloy sample is increased, a pattern of increasing, then decreasing, and then increasing surface roughness is observed in the sample. The surface roughness reaches its highest at  $\theta = 30^\circ$  and its lowest at  $\theta = 45^\circ$ . The lowest surface roughness is 0.3155, 0.2118, and 0.2320  $\mu\text{m}$  from belt grit of P400 to P800, respectively. The belt



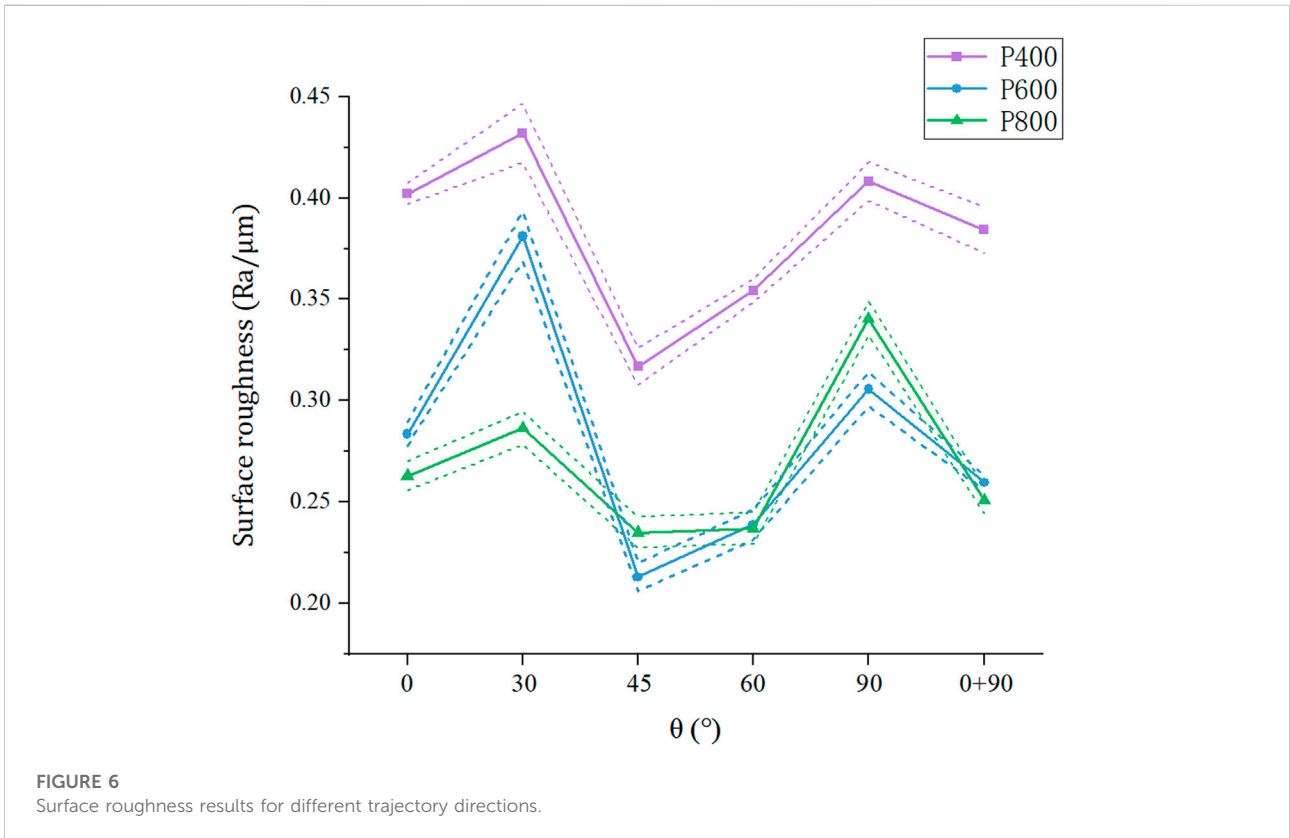
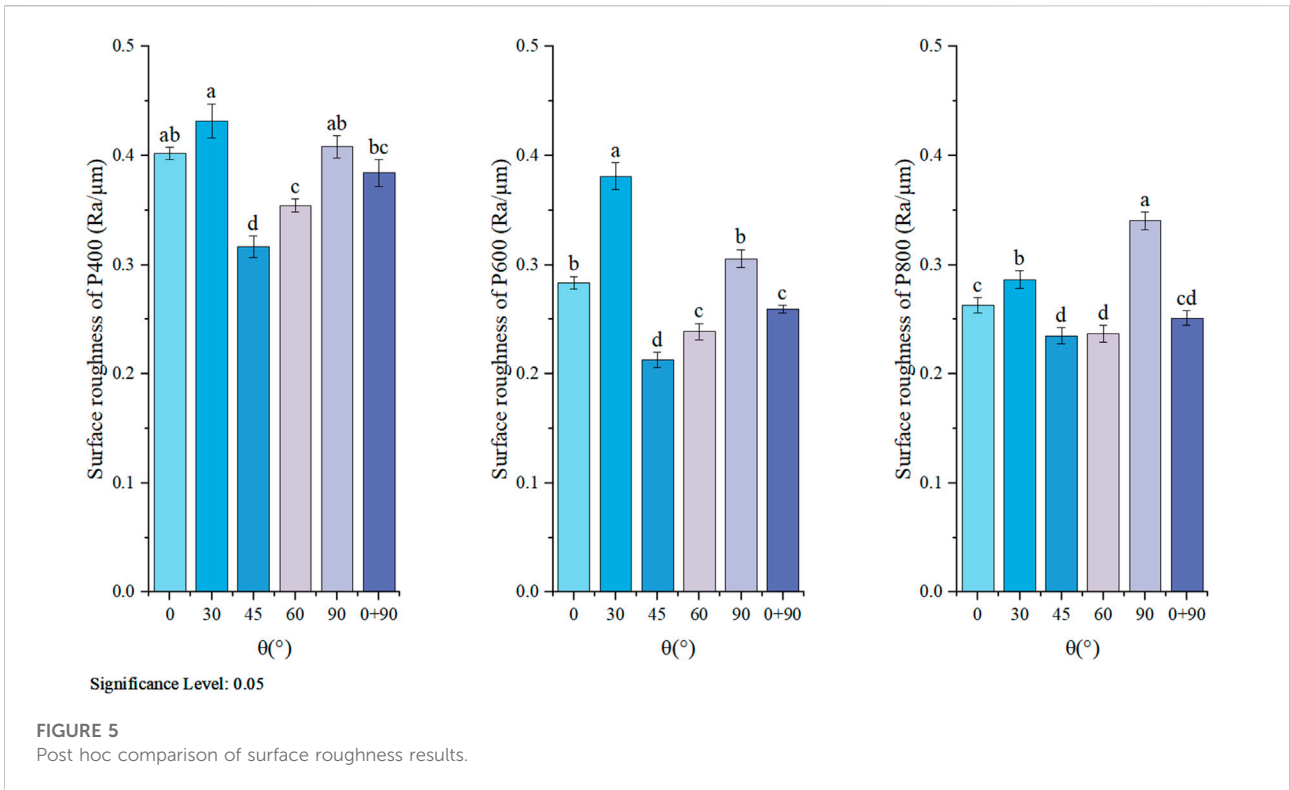
grinding process is essentially the coupling of multiple discrete abrasive grains to the workpiece surface simultaneously. Each grain is simultaneously subjected to the squeezing action of neighbouring grains as it grinds to form a plastic groove, resulting in the formation of new pile-up in the groove (Hu et al., 2022). On a microscopic level, grain orientation affects the inhomogeneity of material slip deformation during the cutting process of the abrasive grains, leading to an increase or decrease in the cutting force of the grains, which ultimately exhibits different surface roughness (Ji et al., 2022). The surface

roughness of the sample is lowest when the grinding track direction satisfies  $\theta = 45^\circ$ . The grain orientation may correspond to the lowest inhomogeneity of material slip deformation, resulting in a relative increase in the abrasive grain cutting force. The abrasive belt grains plough and cut the deepest areas on the workpiece surface, and the grinding material removal is more effective.

Furthermore, one of the data on the far right-hand side of the graph, i.e., grinding in the  $\theta = 0^\circ$  direction followed by a second covering grinding in the  $\theta = 90^\circ$  direction. The results show that two successive grinding in different angular trajectory directions results in lower surface roughness than grinding alone in the  $\theta = 0^\circ$  or  $\theta = 90^\circ$  directions, but still somewhat higher than in the  $\theta = 45^\circ$  direction. This could be because the formation of longitudinal plastic grooves follows the formation of transverse plastic grooves after the first grinding and after the second grinding. In this process, the transverse grooves are partially removed, and longitudinal grooves are formed simultaneously, resulting in a lower surface roughness for  $\theta = 0 + 90^\circ$  compared to the surface roughness for either transverse or longitudinal grooves formed alone. However, the surface roughness is higher this time than at  $\theta = 45^\circ$  due to the stacking effect caused by the increased abrasive grain extrusion caused by superimposed grinding.

### 3.2 Effect of trajectory direction on residual stress

Several studies have shown that compressive residual stresses on surfaces can counteract tensile stresses induced by external loads, retard the expansion of surface cracks, improve fatigue properties, increase wear resistance and improve surface integrity (Peng et al., 2021). All surface residual stress data (Specific data shown in Supplementary Material) obtained from the measurements were divided into three groups by different abrasive belt grit sizes for normality testing and one-way ANOVA to ensure whether the effect of the change in  $\theta$  on the surface residual stress met significance at the 0.05 level. The post hoc comparison results of the ANOVA are shown in Figure 7, which verified that there was some significant difference in the level of surface residual stress caused by different  $\theta$ . The relationship between the surface residual stresses and the  $\theta$  angle of the titanium alloy samples after grinding with different grit sizes are shown in Figure 8. During the grinding process, the residual compressive stress on the sample surface is reduced by the grinding heat. The interaction between the sample and the abrasive grains creates a residual stress field in the grinding area. When grinding is first completed, the sample surface shows a coexistence of compressive and tensile stresses. As the temperature decreases, the tensile residual stresses due to thermal expansion decrease,



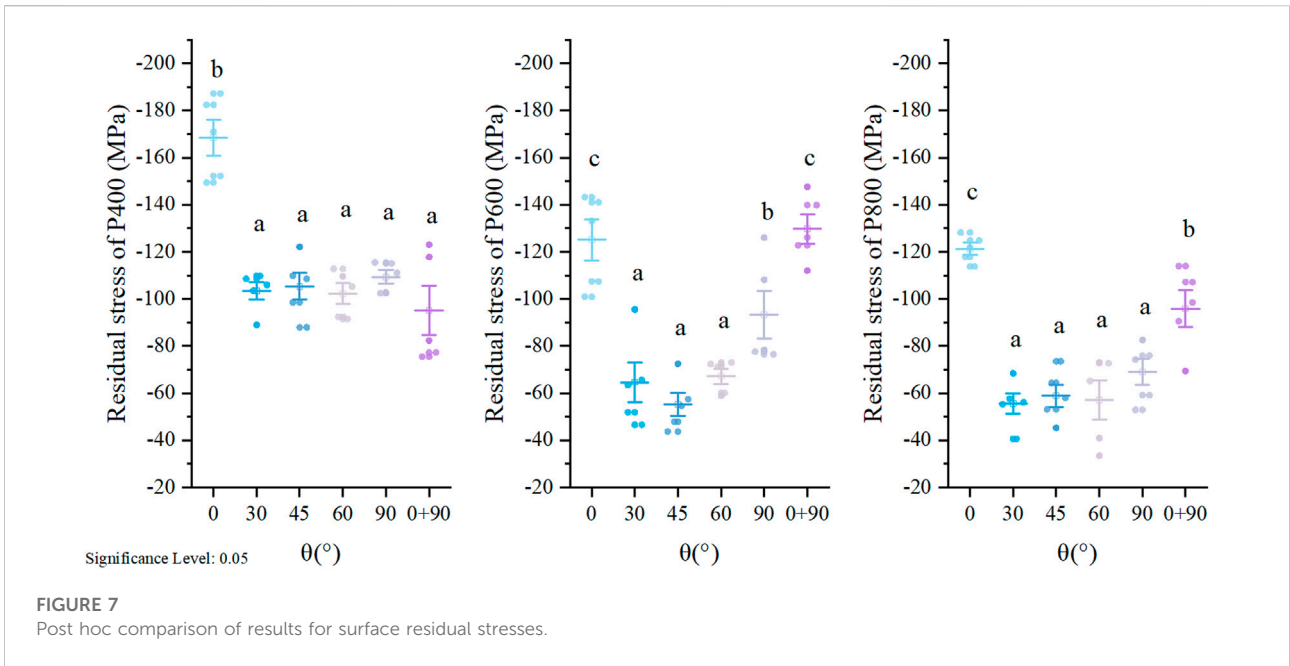


**FIGURE 7**  
Post hoc comparison of results for surface residual stresses.

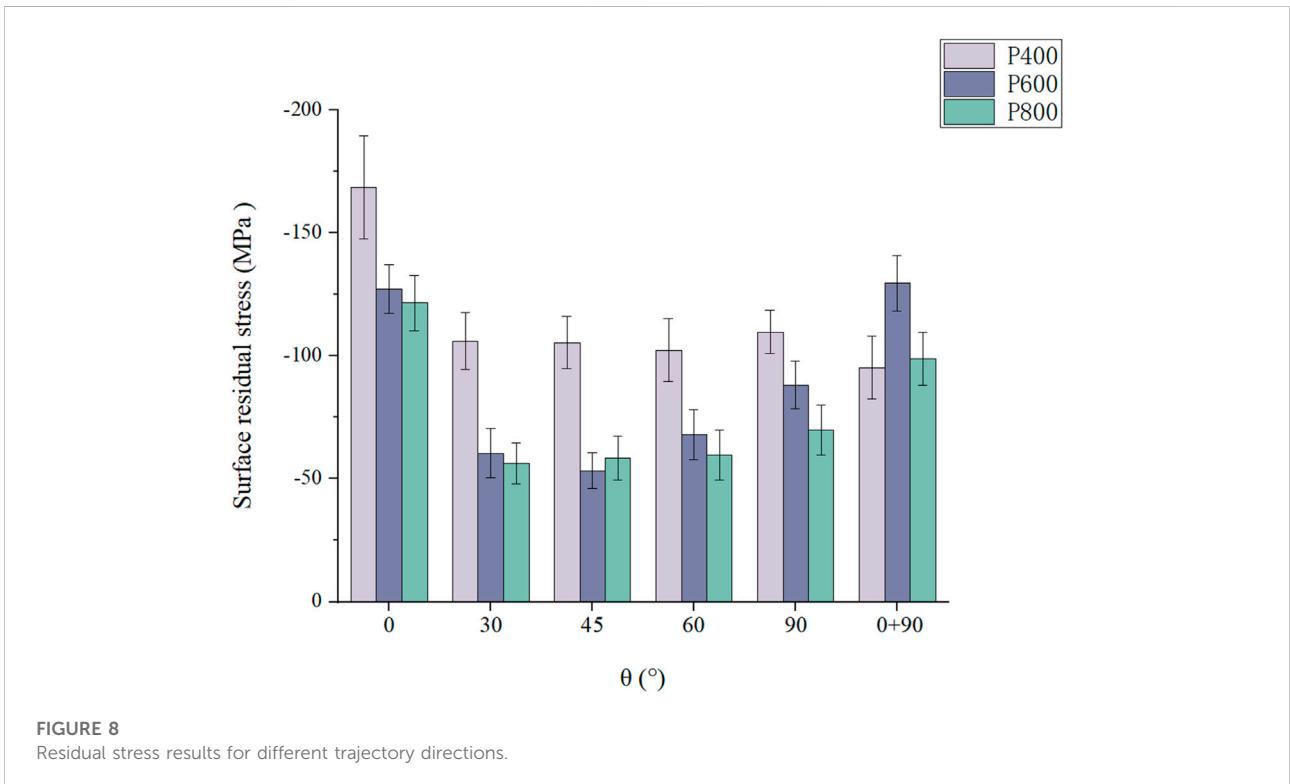
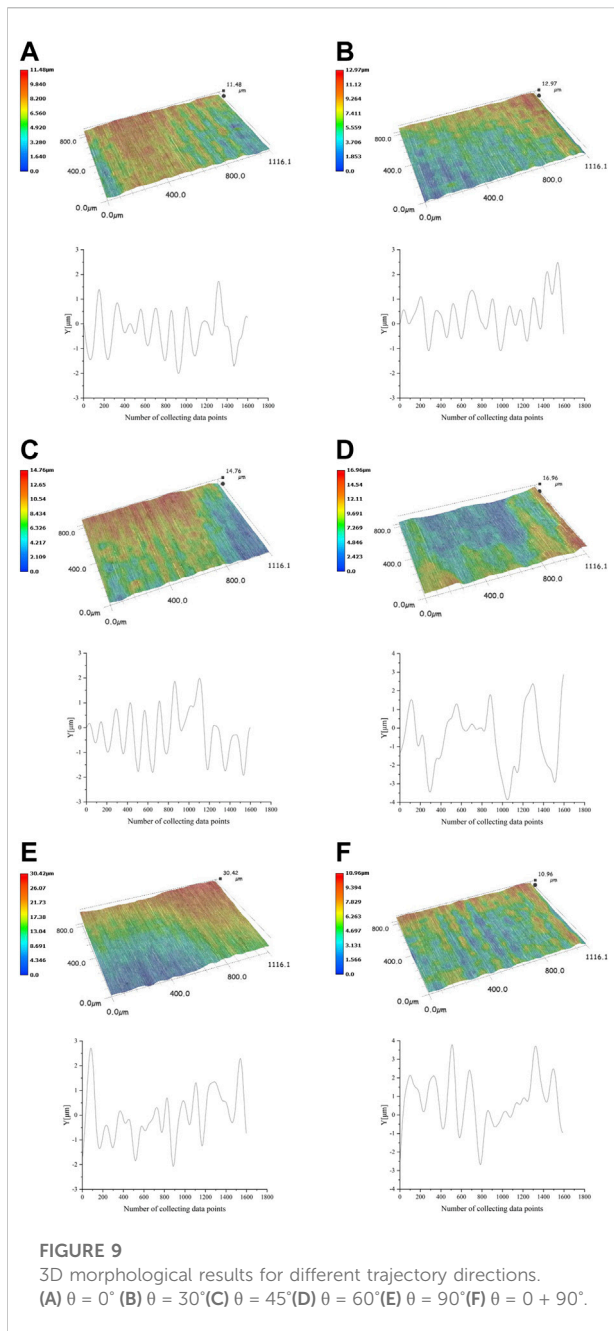


**FIGURE 8**  
Residual stress results for different trajectory directions.

and the sample surface becomes dominated by compressive residual stresses (Wen et al., 2021). Overall, the small value of the grinding depth set in the process parameters leads to a low absolute value of the compressive residual stresses.

As the angle  $\theta$  between the belt grinding direction and the feed direction of the titanium alloy sample increases, the residual stress on the surface of the titanium alloy sample tends to decrease and then increase. The magnitude of the





residual stresses varies from  $-50$  to  $-170$  MPa with the angle  $\theta$ . As the angle  $\theta$  between the belt grinding direction and the feed direction increases, the area of interaction between the abrasive grains and the material surface during belt grinding changes, resulting in different effects of plastic deformation between the abrasive grains and the sample surface due to mechanical and high-temperature effects. Therefore, the residual compressive stress on the surface of the titanium alloy sample regularly decreases or increases. In addition, the residual compressive stress on the surface of the

titanium alloy sample is maximum when the angle  $\theta = 0^\circ$  is used, and the use of the direction  $\theta = 0 + 90^\circ$  does not cause the residual compressive stress on the surface to be greater than that of the angle  $\theta = 0^\circ$  alone. The average residual compressive stress on the surface of titanium alloy samples tends to decrease as the grit size of the abrasive belt increases.

### 3.3 Surface morphology of different grinding trajectories

Micrographs of the test samples' surfaces and 3D morphology were observed using the KEYENCE ultra-deep-field 3D microscope system. Figures 9, 10 show the three-dimensional morphological images and micrographs of the titanium alloy samples after grinding. (A) to (F) represent the angles  $\theta = 0^\circ, 30^\circ, 45^\circ, 60^\circ, 90^\circ$  and  $0 + 90^\circ$  between the grinding direction of the abrasive belt and the feed direction of the titanium alloy sample. As shown in Figure 9, the surface consistency of the titanium alloy samples was excellent at  $\theta = 0^\circ$  and  $\theta = 30^\circ$ . As the angle  $\theta$  increases, the value of height difference shows a trend of rising and then falling. At  $\theta = 60^\circ$ , the height difference reaches its maximum value, and the grinding depth is the greatest, while at  $\theta = 0 + 90^\circ$ , the height difference value and grinding depth are closer to those at  $60^\circ$ .

The plastic deformation produced during material removal is a coupling of mechanical and thermal effects. As a result of the high temperatures experienced in grinding, the metamorphic layer produced on the sample's surface is susceptible to mechanical adhesion, such as chips or abrasive grains, resulting in defects such as craters or cracks (Caudill et al., 2018; Chen et al., 2022). As seen in Figure 10, many plastic grooves and scratches appear on the sample's surface under the squeezing action of the abrasive grains. The surface texture of the sample after grinding is relatively uniform. However, a few areas are distributed with irregularly shaped micro-craters, of which the red line boxes in Figures 10C,D show only a few examples. This was likely due to the frictional wear that occurred during the abrasive belt grinding process when the few abrasive grains of the belt interacted with the titanium alloy material. Due to the poor thermal conductivity of the titanium alloy, micro craters are thus formed to accommodate the abrasive grains under ambient conditions of elevated temperature. As the grinding angle  $\theta$  decreases in size, the ground surface is finer, and the microtexture is more uniform.

As shown in Figures 10D, E, when the grinding trajectory direction satisfies  $\theta = 60^\circ$  and  $\theta = 90^\circ$ . From a macroscopic point of view, more irregularly shaped micro craters can be seen on the surface of the ground sample. This was possibly due to the increased contact area between the abrasive grains on the abrasive belt and the titanium alloy material during an interaction at  $\theta = 60^\circ$  and  $\theta = 90^\circ$ , leading to an increase in

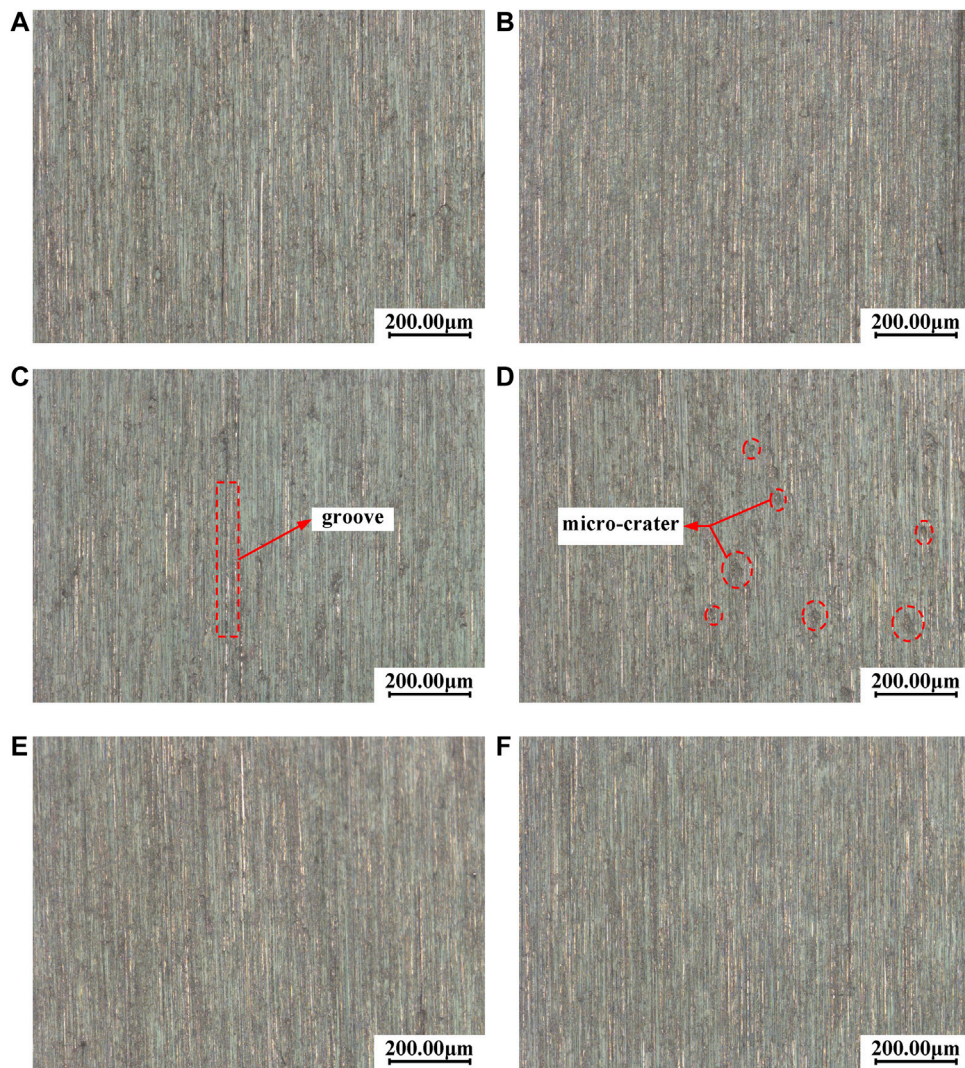


**FIGURE 10**

Micrograph of grinding surface with different trajectory directions. (A)  $\theta = 0^\circ$  (B)  $\theta = 30^\circ$  (C)  $\theta = 45^\circ$  (D)  $\theta = 60^\circ$  (E)  $\theta = 90^\circ$  (F)  $\theta = 0 + 90^\circ$ .

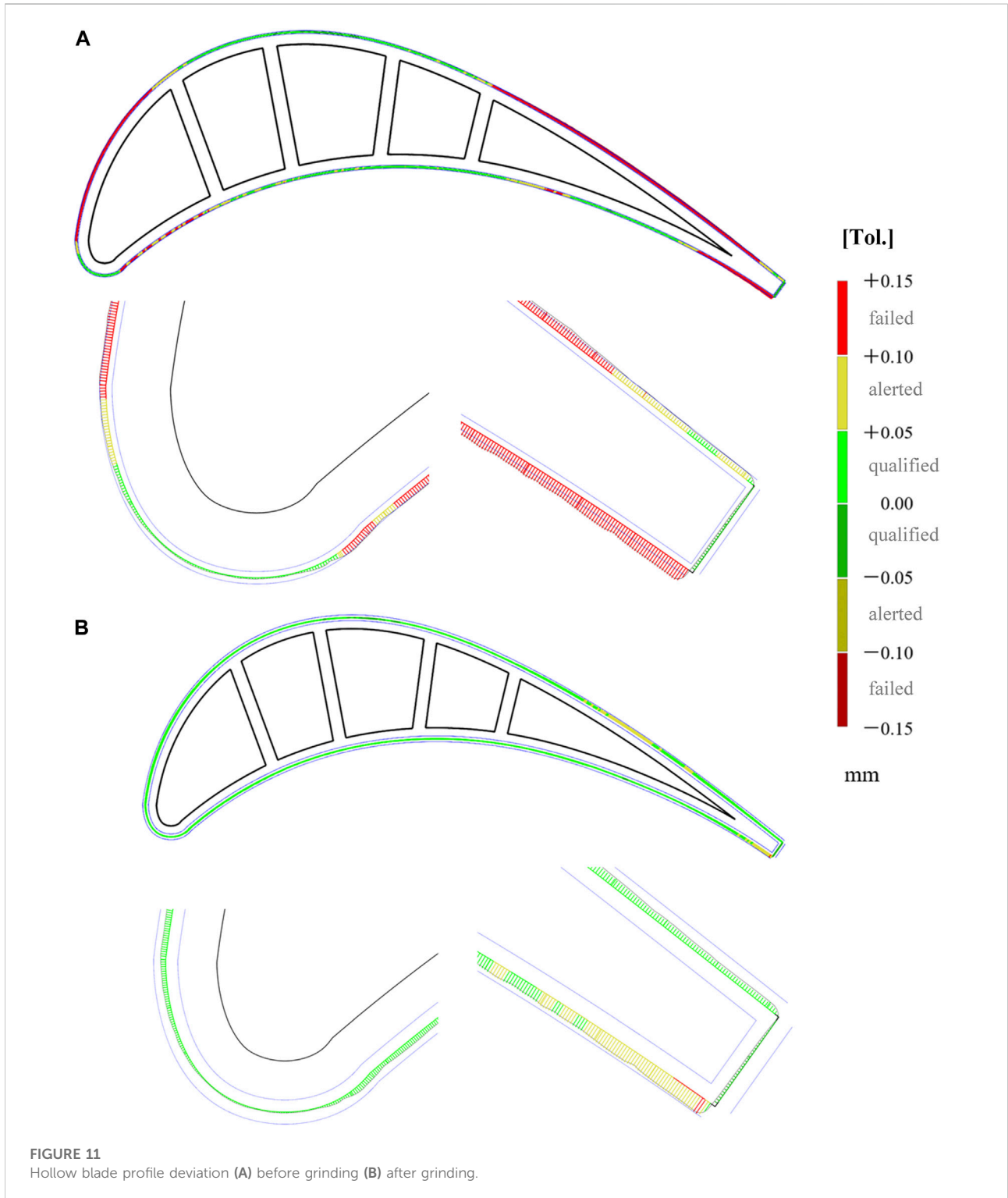
temperature and easier formation of micro craters. From a microscopic point of view, the mechanical and thermal coupling between the abrasive grains and the crystals on the material surface occurs. The angle between the crystal arrangement and the grinding direction changes with the change in the angle  $\theta$ , resulting in a change in grain orientation and morphology on the surface of the sample after the grinding process. Consequently, the crystal slip direction on the material surface is more likely to form a micro-crater. In brief, as the angle  $\theta$  between the grinding direction of the abrasive belt and the feeding direction of the titanium alloy sample changes, the coupling of mechanical and thermal effects on the sample during the grinding process changes, resulting in the formation of a different microscopic surface texture.

### 3.4 Effect of trajectory direction on blade profile accuracy

Verifying the profile accuracy of the hollow blade is a critical way to measure the effectiveness of the abrasive belt grinding trajectory (Lv et al., 2020). The extracted blade samples must have a cross-sectional profile within a tolerance band of  $\pm 0.100$  mm. The blade sample was ground using the grinding process parameters shown in Table 4. The ATOS 5 Airfoil blue profile measuring instrument was used to scan the point cloud information of the sample before and after grinding. The GOM software was used as a platform to carry out model alignment by the ICP algorithm. The hollow blade profile deviation was analysed, and finally, the residual data of the blade before and after the test was

**TABLE 4** Blade test grinding parameters.

Belt grit (#)	Linear velocity (m/s)	Feedrate (mm/min)	Step pitch (mm)	$\theta$ (°)
200	5	10–50	0.2	0



obtained. The profile deviation of the blade sample before and after grinding is shown in Figure 11. The blade section's deviation ranges from 0.034 to 0.184 mm, with an average deviation of 0.115 mm. The blade's cross-section deviations after grinding range from 0.011 to 0.103 mm, with an average deviation value of 0.035 mm. It can be seen that the vast majority of the blade profile deviations are within the tolerance band of  $\pm 0.100$  mm. Only a tiny part of the blade tip has a small grinding volume outside the tolerance zone which may be caused by measurement or machining errors. The range and value of the overrun are small and can be subsequently corrected by additional grinding. It is demonstrated that the proposed belt grinding trajectory planning in this paper can achieve the machining accuracy targets for hollow blades. The actual results show that the blade grinding accuracy is high, further verifying the feasibility and validity of the above grinding results for the titanium alloy hollow blade sample.

## 4 Conclusion

In this work, by proposing a trajectory planning method based on the interaction between the abrasive grains and the material directly during abrasive belt grinding, the effect of the relationship between the grinding direction and the sample feed direction on the surface integrity of titanium alloy hollow blades, including the surface roughness, surface residual stress, surface topography, and contour accuracy, is investigated experimentally in this study. The results of this study will provide a theoretical foundation and technical support for developing abrasive belt grinding technology for the high surface integrity of complex surfaces. Here are the conclusions that have been reached:

First, changing the angle  $\theta$  between the belt grinding direction and the feed direction of the titanium alloy sample significantly affected the surface roughness and the residual stress level. By altering the angle  $\theta$ , the surface roughness of the titanium alloy sample could be reduced by about 40%, and the compressive residual stress on the surface could be increased by about 50%. The surface quality of the ground sample is better with high uniformity of microtexture. Therefore it can effectively improve the surface integrity of titanium alloy hollow blades.

Second, due to the poor thermal conductivity of titanium alloys, considering cooling solutions before machining can avoid high-temperature sparks on the surface during grinding, which can lead to more defects. The direct use of abrasive belts with smaller grit sizes is more beneficial for improving the surface quality of the workpiece, provided that the cost of machining is considered.

In conclusion, the test results of titanium alloy hollow blades show that the relationship between the belt grinding direction and the feed direction of the titanium alloy sample has a particular bearing on the integrity of the surface. Through comprehensive analysis, angle  $\theta = 0^\circ$  was considered to obtain a higher-quality surface. Ground blade profile accuracy can reach the machining precision index of

hollow blades as a further check on the reliability of the surface integrity law for different machining trajectory directions. Using the law proposed in this study to capture further its influence on the surface integrity of complex curved part machining is beneficial. It has a guiding role in improving the surface quality of complex curved parts such as titanium alloy hollow blades.

## Data availability statement

The raw data supporting the conclusion of this article will be made available by the authors, without undue reservation.

## Author contributions

GX and GJ conceived and designed the study. HY, ZZ, and YW performed the experiments. HY wrote the manuscript. GX and GJ reviewed and edited the manuscript. All authors read and approved the manuscript.

## Funding

This work was supported by the National Natural Science Foundation of China (U1908232); the National Science and Technology Major Project [Grant No. 2017-VII-0002-0095]; and the Graduate scientific research and innovation foundation of Chongqing [Grant No. CYB22009].

## Conflict of interest

The authors declare that the research was conducted in the absence of any commercial or financial relationships that could be construed as a potential conflict of interest.

## Publisher's note

All claims expressed in this article are solely those of the authors and do not necessarily represent those of their affiliated organizations, or those of the publisher, the editors and the reviewers. Any product that may be evaluated in this article, or claim that may be made by its manufacturer, is not guaranteed or endorsed by the publisher.

## Supplementary material

The Supplementary Material for this article can be found online at: <https://www.frontiersin.org/articles/10.3389/fmats.2022.1052523/full#supplementary-material>

## References

- Caudill, J., Schoop, J., and Jawahir, I. S. (2018). Correlation of surface integrity with processing parameters and advanced interface cooling/lubrication in burnishing of Ti-6Al-4V alloy. *Adv. Mater. Process. Technol.* 5 (1), 53–66. doi:10.1080/2374068x.2018.1511215
- Chen, G., Caudill, J., Chen, S., and Jawahir, I. S. (2022). Machining-induced surface integrity in titanium alloy Ti-6Al-4V: An investigation of cutting edge radius and cooling/lubricating strategies. *J. Manuf. Process.* 74, 353–364. doi:10.1016/j.jmapro.2021.12.016
- Chen, Z., Shi, Y., Lin, X., Yu, T., Zhao, P., and Kang, C. (2019). Experimental investigation of effects of polishing process on surface residual stress of TC4 blade based on sensitivity analysis. *Exp. Tech.* 43 (6), 729–738. doi:10.1007/s40799-019-00333-z
- Guo, J., Shi, Y. Y., Chen, Z., Yu, T., Zhao, P., and Shirinzadeh, B. (2019). Optimal parameter selection in robotic belt polishing for aeroengine blade based on GR-RSM method. *Symmetry (Basel)*. 11 (12), 1526. doi:10.3390/sym11121526
- Hou, N., Wang, M. H., Wang, B., Zheng, Y. H., Zhou, S. Y., and Song, C. (2022). Fundamental functions of physical and chemical principles in the polishing of titanium alloys: Mechanisms and problems. *Int. J. Adv. Manuf. Technol.* 118 (7–8), 2079–2097. doi:10.1007/s00170-021-08100-4
- Hu, Z., Chen, Y., Lai, Z., Yu, Y., Xu, X., Peng, Q., et al. (2022). Coupling of double grains enforces the grinding process in vibration-assisted scratch: Insights from molecular dynamics. *J. Mater. Process. Technol.* 304, 117551. doi:10.1016/j.jmatprotec.2022.117551
- Ji, H., Song, Q., Du, Y., Zhao, Y., and Liu, Z. (2022). Grain-scale material removal mechanisms of crystalline material micro-cutting. *Int. J. Mech. Sci.* 233, 107671. doi:10.1016/j.ijmecsci.2022.107671
- Kalantari, O., Jafarian, F., and Fallah, M. M. (2021). Comparative investigation of surface integrity in laser assisted and conventional machining of Ti-6Al-4 V alloy. *J. Manuf. Process.* 62, 90–98. doi:10.1016/j.jmapro.2020.11.032
- Li, C., Hu, Y., Zhang, F., Geng, Y., and Meng, B. (2022). Molecular dynamics simulation of laser assisted grinding of GaN crystals. *Int. J. Mech. Sci.* 239, 107856. doi:10.1016/j.ijmecsci.2022.107856
- Li, L., Ren, X., Feng, H., Chen, H., and Chen, X. (2021). A novel material removal rate model based on single grain force for robotic belt grinding. *J. Manuf. Process.* 68, 1–12. doi:10.1016/j.jmapro.2021.05.029
- Liang, Q., Shan, K., and Li, Z. (2020). Investigation of grain wear in diamond abrasive belt grinding titanium alloy blade for aeroengine. *Diamond & Abrasives Engineering* 40 (4), 59–64. doi:10.13394/j.cnki.jgszz.2020.4.0009
- Lin, X. J., Wu, D. B., Shan, X. F., Wu, G., Cui, T., Zhang, Y., et al. (2018). Flexible CNC polishing process and surface integrity of blades. *J. Mech. Sci. Technol.* 32 (6), 2735–2746. doi:10.1007/s12206-018-0530-0
- Liu, D., Shi, Y. Y., Lin, X. J., Xian, C., and Gu, Z. Y. (2020). Polishing surface integrity of TC17 aeroengine blades. *J. Mech. Sci. Technol.* 34 (2), 689–699. doi:10.1007/s12206-020-0114-7
- Liu, S., Xiao, G., Lin, O., He, Y., and Song, S. (2023). A new one-step approach for the fabrication of microgrooves on Inconel 718 surface with microporous structure and nanoparticles having ultrahigh adhesion and anisotropic wettability: Laser belt processing. *Appl. Surf. Sci.* 607, 155108. doi:10.1016/j.apsusc.2022.155108
- Lv, Y. J., Peng, Z., Qu, C., and Zhu, D. H. (2020). An adaptive trajectory planning algorithm for robotic belt grinding of blade leading and trailing edges based on material removal profile model. *Robotics Computer-Integrated Manuf.* 66, 101987. ARTN 101987. doi:10.1016/j.rcim.2020.101987
- Palaniyappan, S., Veiravan, A., Kumar, V., Mathusoothanaperumal Sukanya, N., and Veeman, D. (2022). Process optimization and removal of phenol formaldehyde resin coating using mechanical erosion process. *Prog. Rubber, Plastics Recycl. Technol.* 38 (2), 141–154. doi:10.1177/14777606211066316
- Peng, Z., Zhang, X., and Zhang, D. (2021). Improvement of Ti-6Al-4V surface integrity through the use of high-speed ultrasonic vibration cutting. *Tribol. Int.* 160, 107025. doi:10.1016/j.triboint.2021.107025
- Pushp, P., Dasharath, S. M., and Arati, C. (2022). Classification and applications of titanium and its alloys. *Mater. Today Proc.* 54, 537–542. doi:10.1016/j.matpr.2022.01.008
- Rangasamy, N., Rakurty, C. S., and Balaji, A. K. (2022). A multiscale study on machining induced surface integrity in Ti-6Al-4V alloy. *Procedia CIRP* 108, 787–792. doi:10.1016/j.procir.2022.03.122
- Sabarinathan, P., Annamalai, V. E., and Xavier Kennedy, A. (2020). On the use of grains recovered from spent vitrified wheels in resinoid applications. *J. Mater. Cycles Waste Manag.* 22 (1), 197–206. doi:10.1007/s10163-019-00927-0
- Tan, L., Yao, C. F., Zhang, D. H., Ren, J. X., Zhou, Z., and Zhang, J. Y. (2020). Evolution of surface integrity and fatigue properties after milling, polishing, and shot peening of TC17 alloy blades. *Int. J. Fatigue* 136, 105630. ARTN 105630. doi:10.1016/j.ijfatigue.2020.105630
- Tao, Z., Yaoyao, S., Laakso, S., and Zhou, J. M. (2017). Investigation of the effect of grinding parameters on surface quality in grinding of TC4 titanium alloy. *Procedia Manuf.* 11, 2131–2138. doi:10.1016/j.promfg.2017.07.344
- Wang, Y., Xiu, S., and Zhang, S. (2021). Microstructure evolution and crystallographic slip modes during grind hardening in TC21 titanium alloy. *Surf. Coatings Technol.* 417, 127211. doi:10.1016/j.surfcoat.2021.127211
- Wen, J., Tang, J., and Zhou, W. (2021). Study on formation mechanism and regularity of residual stress in ultrasonic vibration grinding of high strength alloy steel. *J. Manuf. Process.* 66, 608–622. doi:10.1016/j.jmapro.2021.04.040
- Xu, M., Li, C., Kurniawan, R., Park, G., Chen, J., and Ko, T. J. (2022). Study on surface integrity of titanium alloy machined by electrical discharge-assisted milling. *J. Mater. Process. Technol.* 299, 117334. doi:10.1016/j.jmatprotec.2021.117334
- Yi, J., Zhou, W., and Deng, Z. H. (2019). Experimental study and numerical simulation of the intermittent feed high-speed grinding of TC4 titanium alloy. *Metals* 9 (7), 802. ARTN 802. doi:10.3390/met9070802
- Zhang, J. J., Liu, J., and Yang, S. Q. (2022). Trajectory planning of robot-assisted abrasive cloth wheel polishing blade based on flexible contact. *Int. J. Adv. Manuf. Technol.* 119 (11–12), 8211–8225. doi:10.1007/s00170-022-08737-9
- Zhu, S., Xiao, G., He, Y., Liu, G., Song, S., and Jiahua, S. (2022). Tip vortex cavitation of propeller bionic noise reduction surface based on precision abrasive belt grinding. *J. Adv. Manuf. Sci. Technol.* 2 (1), 2022003. doi:10.51393/j.jamst.2022003
- Zhu, W.-L., and Beaucamp, A. (2020). Compliant grinding and polishing: A review. *Int. J. Mach. Tools Manuf.* 158, 103634. doi:10.1016/j.ijmactools.2020.103634